2-1-1992

# Effect of CO2 on the Processing of Y-Ba-Cu-O Superconductors

C. Zhang
*San Jose State University*

Guna S. Selvaduray
*San Jose State University*, gunas@email.sjsu.edu



## Recommended Citation

C. Zhang and Guna S. Selvaduray. "Effect of CO2 on the Processing of Y-Ba-Cu-O Superconductors" *Journal of Materials Research* (1992): 283-291. https://doi.org/10.1557/JMR.1992.0283

# Effect of $CO_2$ on the processing of Y–Ba–Cu–O superconductors

G. Selvaduray and C. Zhang
*Department of Materials Engineering, San Jose State University, San Jose, California 95192-0086*

U. Balachandran, Y. Gao, K. L. Merkle, H. Shi, and R. B. Poeppel
*Materials and Components Technology Division, Argonne National Laboratory, 9700 South Cass Avenue, Argonne, Illinois 60439-4838*

(Received 26 June 1991; accepted 10 September 1991)

The superconducting properties of $YBa_2Cu_3O_{6+x}$ reacted with various known ratios of $O_2/CO_2$ gas mixtures during sintering at different temperatures were studied. $J_c$ was found to decrease drastically upon reaction with $CO_2$, becoming zero at certain $CO_2$ activities. The stability region for the 123 superconductor, as a function of $CO_2$ activity and temperature, was empirically formulated as follows: $\log\ p_{CO_2} < (-45{,}000)/T + 33.4$. The grain boundaries in sintered samples with $J_c = 0$ were investigated with HRTEM in conjunction with EDS. Two distinct types of grain boundaries were observed. Approximately 10% of the grain boundaries were wet by a thin layer of a second phase, deduced to be $BaCuO_2$. The remaining boundaries were sharp grain boundaries. The grain structure near the sharp grain boundaries was tetragonal. These two types of grain boundaries are thought to be responsible for $J_c$ being zero.

## I. INTRODUCTION

There are two potential sources of $CO_2$ when $YBa_2Cu_3O_{6+x}$ (123) superconductors are processed by solid-state sintering. One source is the $CO_2$ contained in the oxygen gas used during sintering and/or annealing. Another source is the $CO_2$ derived from the decomposition of $BaCO_3$ during the calcination step. Each source affects the quality of the final product in different ways and can lead to a drop in the critical current density, $J_c$.

During calcination, the $Y_2O_3$, $BaCO_3$, and CuO powders ideally react according to reactions (1) and (2), to form 123.

$$BaCO_3\ (s) + CuO\ (s) \rightarrow CO_2\ (g) + BaCuO_2\ (s) \quad (1)$$

$$4BaCuO_2\ (s) + Y_2O_3(s) + 2CuO\ (s) \rightarrow 2YBa_2Cu_3O_x\ (s) \quad (2)$$

When $BaCO_3$ decomposes, according to reaction (1), $CO_2$ is released. The localized concentration of $CO_2$ can quickly reach its equilibrium value, and stagnant regions of $CO_2$ can form, even in systems with flowing gases. This localized $CO_2$ pressure, depending on the temperature and other thermodynamic conditions, can cause other decomposition reactions, thereby forming undesired phases, which in turn contribute to reduce the critical current density of the final product.

Fjellvåg[1] studied the interaction between $CO_2$ and $YBa_2Cu_3O_{6+x}$ at a total pressure of 1 atm, with 0.999 atm of $O_2$ and 0.001 atm of $CO_2$, and reported two reaction mechanisms:

$$YBa_2Cu_3O_{6+x}\ (s) + 2CO_2\ (g) \rightarrow 2BaCO_3(s) + \tfrac{1}{2}Y_2O_3(s) + 3CuO\ (s) + (2x-1)/4O_2\ (g) \quad (3)$$

$$YBa_2Cu_3O_{6+x}\ (s) + 2CO_2\ (g) \rightarrow 2BaCO_3(s) + \tfrac{1}{2}Y_2Cu_2O_5\ (s) + 2CuO\ (s) + (2x-1)/4O_2\ (g) \quad (4)$$

Reaction (3) was reported to occur at temperatures below 730 ± 10 °C, and reaction (4) at temperatures above 730 ± 10 °C. Both of these reactions lead to the formation of nonsuperconducting phases. As can be seen from these two reactions, the partial pressure of $CO_2$ will determine the extent to which the nonsuperconducting reaction products are formed. The effect of $CO_2$ partial pressure on the oxide-carbonate equilibrium, as a function of temperature, was also derived by Fjellvåg, and is shown in Fig. 1. Analytically, the equilibrium partial pressure of $CO_2$ can be represented by the following expression:

$$\log\ p_{CO_2} = \frac{-8900}{T} + 5.7 \quad (5)$$

where $p_{CO_2}$ is in atmospheres and the temperature $T$ is above 730 °C.

The partial pressure of $CO_2$ can also affect the partial pressure of $O_2$, which in turn affects the oxygen content of the 123 compound formed, and thus the phase composition of the 123.

The superconducting properties of 123 compounds, as a function of oxygen content, have been studied by other investigators.[2–4] For $x \approx 1$, $YBa_2Cu_3O_{6+x}$ is in the orthorhombic phase and exhibits superconductivity at 90 K. As the oxygen content, which is dependent on both temperature and oxygen partial pressure, decreases, the transition temperature of the orthorhombic phase

  

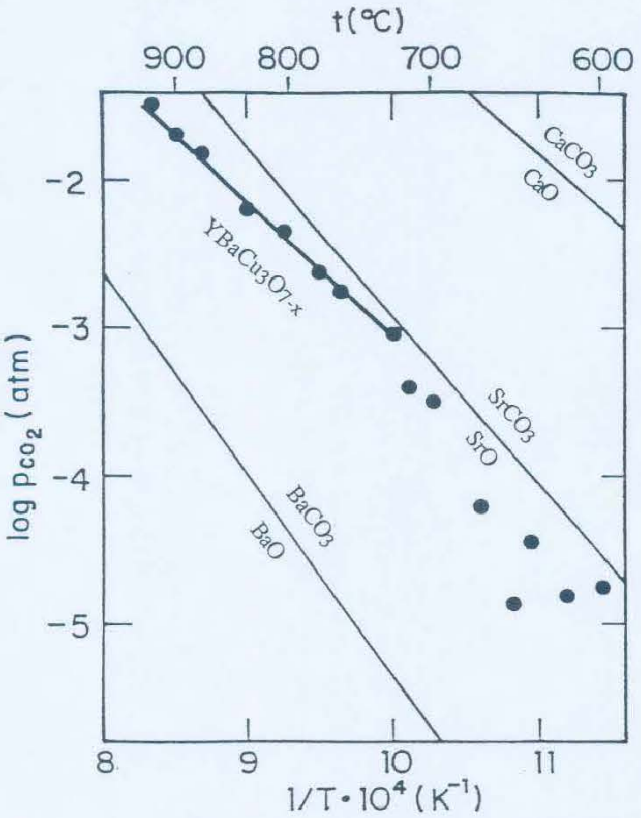


FIG. 1. Stability of $YBa_2Cu_3O_{6+x}$ with respect to carbonate formation ($p_{CO_2}$ + 1 atm).[1]

decreases to 60 K, at $0.6 < x < 0.7$. At $x \approx 0.4$, the material becomes tetragonal, and superconductivity is destroyed. The transition of the orthorhombic phase to the tetragonal phase occurs at an oxygen content of $x \approx 0.5$. The equilibrium constant for reactions (3) and (4) is given by:

$$K = \left\{[p_{O_2}]^{(2x-1)/4}\right\} \Big/ \left\{[p_{CO_2}]^2\right\} \qquad (6)$$

Equation (6) shows the effect of partial pressure of $CO_2$ on the partial pressure of $O_2$, and thus on the structure of the 123 compound synthesized.

This investigation was undertaken to determine the effect of the presence of $CO_2$ in atmospheres used for processing 123 compounds. The specific aims of the investigation included (a) determining process conditions necessary for avoiding the formation of undesirable phases, and (b) establishing processing-structure-properties relationships.

## II. EXPERIMENTAL PROCEDURE

Appropriate amounts of $Y_2O_3$, $BaCO_3$, and CuO were mixed as a 400 gm batch and wet milled for 15 h in methanol in polyethylene jars containing $ZrO_2$ grinding media. The resultant slurry was pan dried and screened through a 30 mesh sieve. The screened powder was calcined for 4 h in flowing $O_2$ with a pressure of ≈2 mm Hg at a temperature of ≈850 °C. During cooling, the vacuum was discontinued, and ambient pressure $O_2$ was passed through. A 3 h hold at 450 °C was incorporated into the cooling schedule to promote oxygenation of the powder. The calcined powders were ground, milled, and checked for phase purity by x-ray diffraction (XRD) and differential thermal analysis (DTA). The calcination procedure used in this work gives essentially phase-pure orthorhombic 123 powder.[5] The calcined powder was cold-pressed into ≈1 cm diameter pellets at ≈ 140 MPa, subdivided into groups, and sintered for 5 h.

Four groups, each made up of four samples, were sintered at temperatures of 910, 940, 970, and 1000 °C, respectively, with oxygen gas at ambient pressure passed through the furnace during the entire process. Sixteen groups, each made up of four samples, were also sintered at the same temperatures, but with $CO_2/O_2$ gas mixtures, at ambient pressure. The $CO_2$ concentration in the mixtures ranged from ≈50 ppm to 5%.

Bars of 1 $mm^2$ cross section and 10 mm long were cut from each pellet for critical current density ($J_c$) measurements. A criterion of 1 $\mu$V/cm was applied to $J_c$ measurements. Representative samples were used for measuring the critical transition temperature ($T_c$) by resistivity and low field RF SQUID magnetometer.

Samples were also mounted and polished, using a diamond paste, down to 1 $\mu$m, for optical and scanning electron microscopy. The mean grain size of each sample was measured using the line intercept method. High resolution transmission electron microscopy (HRTEM) was used for studying the microstructure and composition of the grains and grain boundaries. Phase composition of the sintered samples was studied by XRD.

Finally, the samples that had been sintered in 50 ppm, 500 ppm, and 0.5% $CO_2$ containing atmospheres were reannealed in pure oxygen flow, at 450 °C for 15 h, to check the reversibility of the second phases formed. Samples that had been sintered in pure oxygen flow were reannealed in oxygen flow, with 5% $CO_2$ for 10 h, to check for formation of second phases.

## III. RESULTS

### A. Sintering temperature and atmosphere

The effects of sintering temperature and atmosphere on the density and the critical current density of the samples tested are shown in Figs. 2 and 3, respectively. Figure 2 shows that the sintering temperature has a major effect on the density of the sample, as can be expected. However, the sintering atmosphere, within the range investigated in this work, does not appear to affect the density. The critical current density, on the other hand,

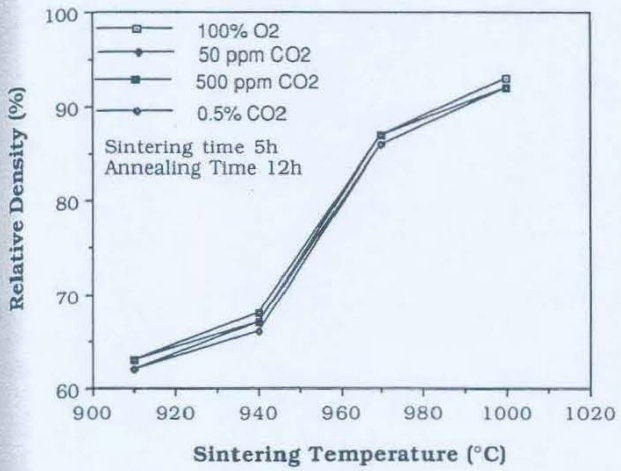


FIG. 2. The effect of sintering temperature on density.

was found to be affected by both sintering temperature and $CO_2$ content in the sintering atmosphere, as shown in Fig. 3. $J_c$ values decreased with decreasing sintering temperature and increasing $CO_2$ content. Figure 4 summarizes these results and presents them in terms of processing conditions, namely $p_{CO_2}$ and $T$, necessary for production of superconductors. The solid line separates the stability regions of superconductors and semiconductors. An experimental relationship between $p_{CO_2}$ and $T$ was derived from this diagram, and found to be as follows:

$$\log\ p_{CO_2} = C/T + D \qquad (7)$$

where $C = -45{,}000$ K and $D = 33.4$.

### B. Microstructure and atmosphere

The microstructures of two typical samples are shown in Figs. 5 and 6. In Fig. 5 the microstructures of samples sintered at 910, 940, 970, and 1000 °C, and 100% $O_2$ are shown. The grain size as determined by

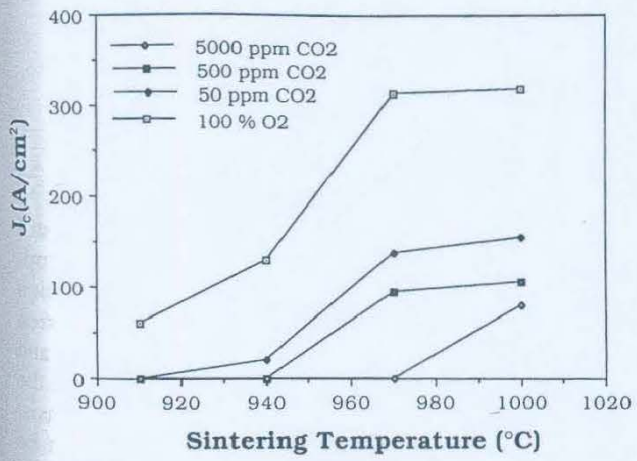


FIG. 3. The effect of sintering temperature on $J_c$.

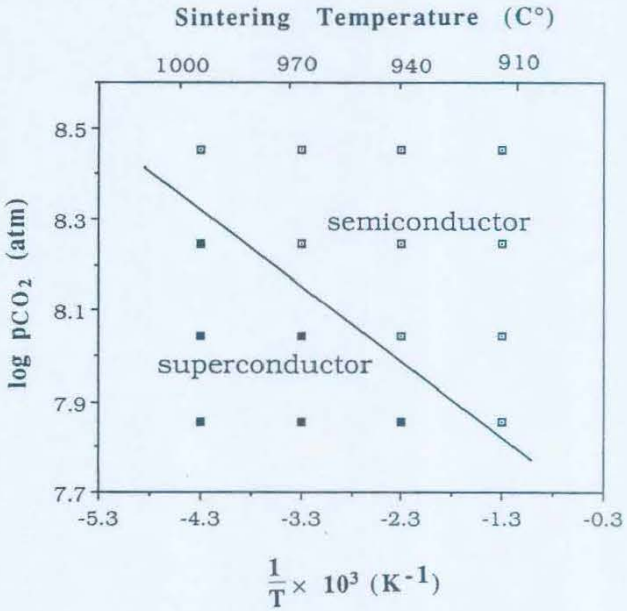


FIG. 4. Stability of 123 compounds as a function of $p_{CO_2}$ and temperature.

the line intercept method is plotted in Fig. 7. Large grain growth is observed at 970 °C, and the grain size data are in good agreement with the density and $J_c$ data reported earlier in Figs. 2 and 3. The denser samples have larger grain sizes, and the $J_c$ increase is thought to result from the increase in connectivity between the grains. From Fig. 6 it can also be seen that the crystals of the samples sintered in lower $CO_2$ atmospheres are twinned, whereas those sintered in 5% $CO_2$ do not show any twinning. The twin structure in 123 determines its orthorhombic superconducting properties,[6] and it can be concluded that the samples sintered in 5% $CO_2$ are not orthorhombic. Close examination of the microstructure also shows that the extent to which the orthorhombic structure is present decreases with increasing $CO_2$ presence in the sintering atmosphere.

### C. Relationship between $T_c$ and atmosphere

The critical temperature, $T_c$, of the samples was measured by both resistivity and magnetization techniques, and are shown in Figs. 8 and 9, respectively. The data in Fig. 8(a), for a sample sintered at 940 °C and 100% $O_2$, exhibits onset of transition at 90 K and zero resistance at 82 K. A linear temperature dependence of resistivity ($R$), with $\delta R/\delta T > 0$ before the onset of superconductivity, indicates that this sample is a good superconductor. Figure 8(b) shows the data for a sample sintered in an atmosphere containing 50 ppm $CO_2$. Two transition temperatures, one at 90 K and one at 80 K, are observed, indicating the presence of a second superconducting transition (or phase), and zero resistance is observed at 78 K. For samples sintered in an atmosphere containing 0.5%

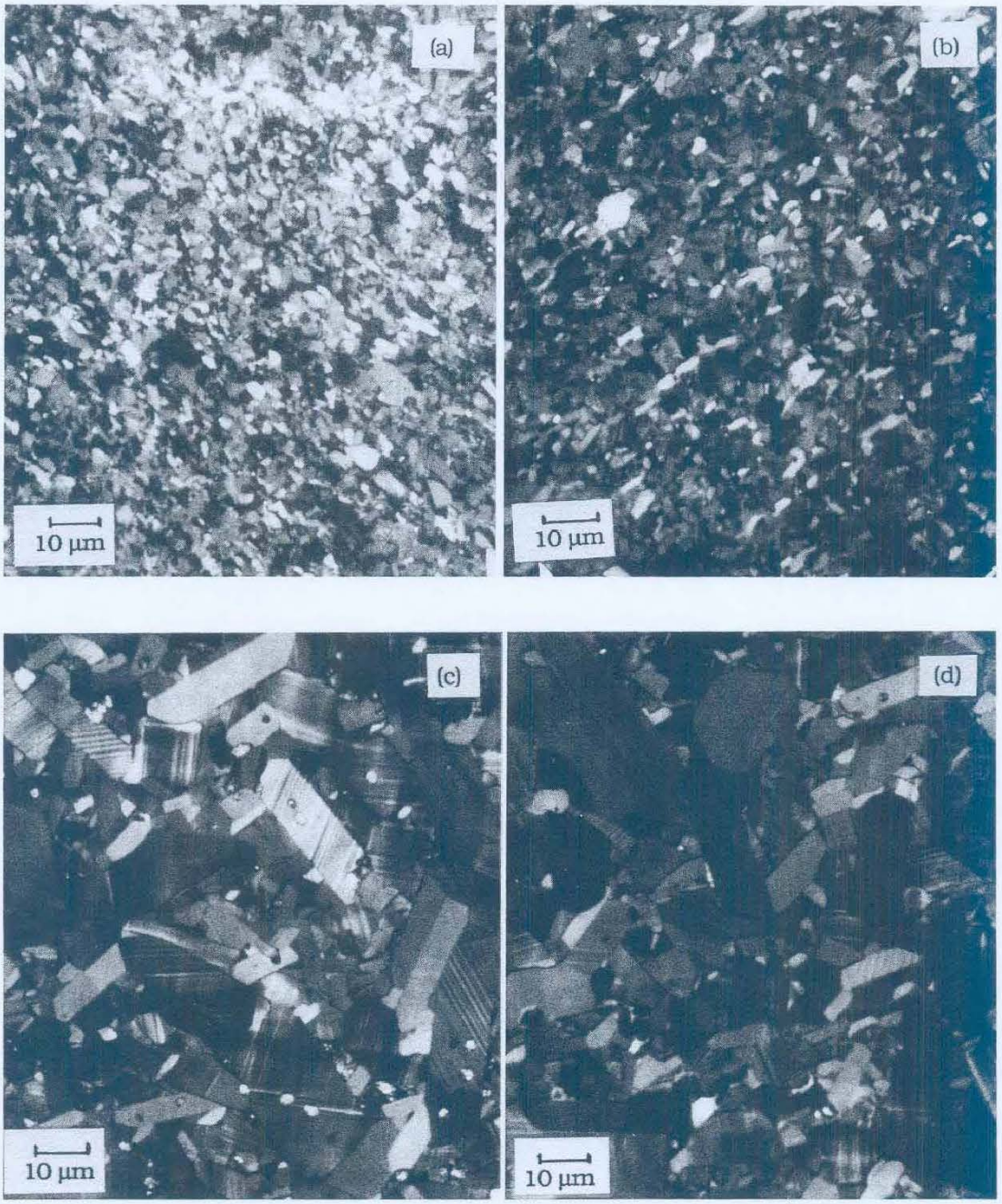


FIG. 5. Optical micrographs for samples sintered under 100% $O_2$ at (a) 910 °C, (b) 940 °C, (c) 970 °C, and (d) 1000 °C.

$CO_2$, $\delta R/\delta T < 0$ [Fig. 8(c)], and the sample shows marked semiconducting characteristics. Increasing $CO_2$ contents in the sintering atmosphere were found to increase the electrical resistivity of the sample. These findings are in good agreement with the findings of Wang *et al.*,[7] Nakazawa and Ishikawa,[8] and Kwok *et al.*[9]

The diamagnetism observed in the data reported in Fig. 9 indicates that the major phase of these samples is still superconducting. The presence of $CO_2$ is found to be detrimental, despite the fact that the major phases are still superconducting. The decrease in superconducting properties is found to be directly related to the concentration of $CO_2$ in the sintering atmosphere. It can be inferred that $CO_2$ leads to partial carbonation of the sample, and that these carbonated phases may accumulate along the grain boundaries. Thus, although these samples consist of superconducting grains, these grains would then be isolated by nonsuperconducting second phases along

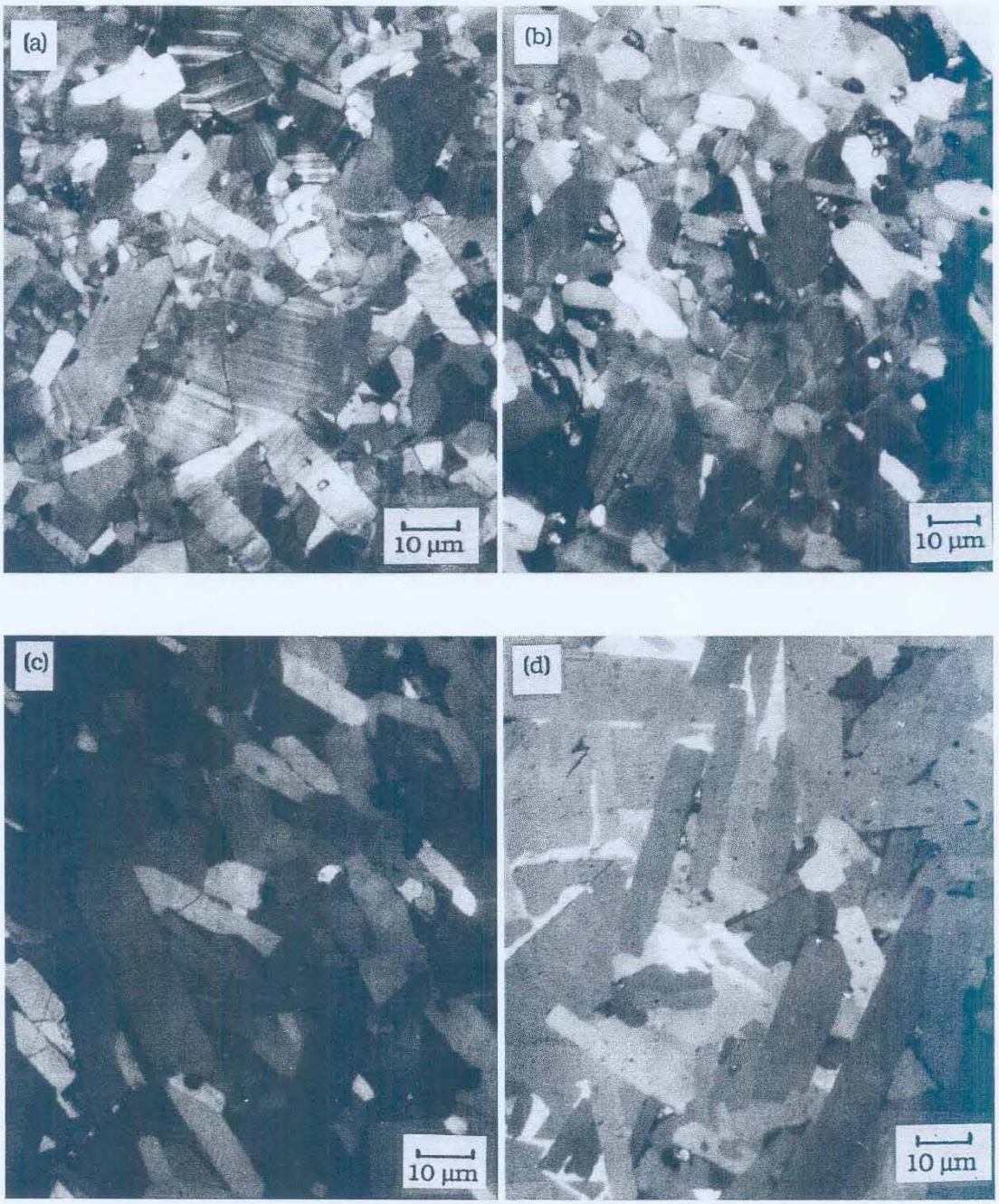


FIG. 6. Optical micrographs for samples sintered at 1000 °C, with (a) pure $O_2$, (b) $O_2$ + 50 ppm $CO_2$, (c) $O_2$ + 0.5% $CO_2$, and (d) $O_2$ + 5% $CO_2$.

the grain boundaries which would cause the $J_c$ value to decrease strongly. This hypothesis was checked by transmission electron microscopy (TEM).

### D. Microstructure and composition determined by TEM

The compositions at and near grain boundaries in typical sintered samples were investigated using TEM in conjunction with energy dispersive spectroscopy (EDS). No evidence of second phases at grain boundaries was found in samples sintered in a 100% $O_2$ atmosphere. However, two distinct types of grain boundaries were observed in the samples that were sintered in 0.5% $CO_2$ + 99.5% $O_2$. Approximately 10% of the grain boundaries were found to be wet by a thin layer of a second phase, as shown in Fig. 10. EDS spectra obtained

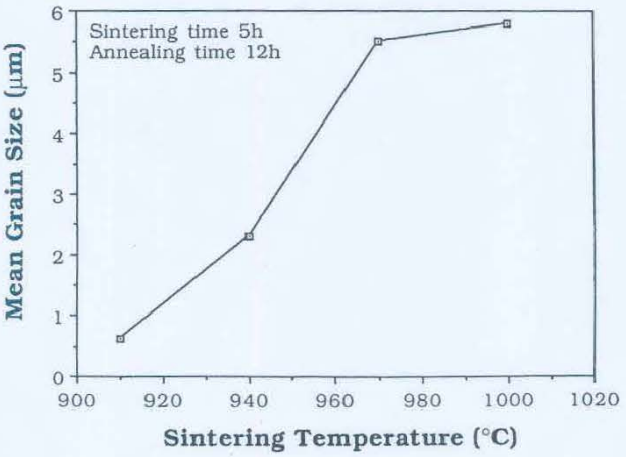


FIG. 7. Grain size of samples sintered under 100% $O_2$.

from locations along this boundary indicated that the composition of this layer was rich in barium and copper, but depleted in yttrium, and was likely to be $BaCuO_2$. At some locations this layer was found to be extremely rich in copper, and it is likely that the composition may be due to the eutectic reaction between $BaCuO_2$ and CuO, in accordance with the phase diagram.[10] The remaining boundaries were sharp grain boundaries, and free from the presence of second phases.

By using high-resolution transmission electron microscopy (HRTEM), it was also found that the structure near the sharp grain boundaries was not orthorhombic, but tetragonal, as shown in Fig. 11. The lattice fringes in the [001] direction were clearly observed, and it was found that $c = 1.19$ nm near the grain boundary whereas $c = 1.17$ nm in the region far from the grain boundary. From neutron diffraction data[11] it is known that $c = 1.19$ nm for the tetragonal structure and $c = 1.17$ nm for the orthorhombic structure. The region having $c = 1.17$ nm was also found to have twin structures, whereas the region having $c = 1.19$ nm was found to have no twins. A boundary could be observed between these two regions. The orthorhombic phase exhibits twinning, but the tetragonal phase does not.[12] This was used as further evidence to conclude that the region adjacent to the grain boundaries is tetragonal, while the region farther away is orthorhombic.

EDS also revealed the presence of precipitates of $Y_2BaCuO_5$ ("211") for the samples sintered in 0.5% $CO_2$, as shown in Fig. 12. Based on the findings here, and the fact that the samples were phase pure before they were sintered, it can be concluded that the 123 compound decomposes in the presence of $CO_2$, yielding $Y_2BaCuO_5$, $BaCO_3$, and CuO.

For samples sintered in 5% $CO_2 + O_2$, the initial 123 phase was found to be completely decomposed. Both EDS and XRD showed that the decomposition products were 211, $BaCO_3$, and CuO.

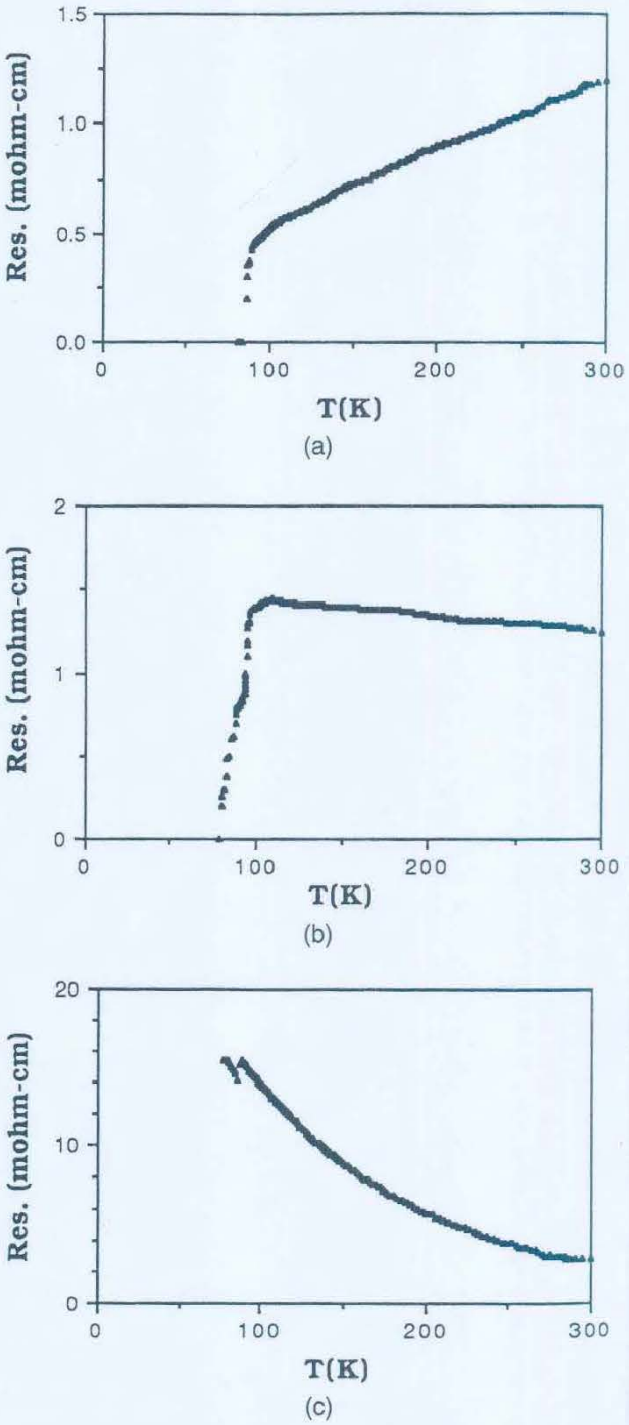


FIG. 8. Resistivity versus temperature for samples sintered at 940 °C, with (a) pure $O_2$, (b) $O_2$ + 50 ppm $CO_2$, and (c) $O_2$ + 0.5% $CO_2$.

## IV. DISCUSSION OF RESULTS

### Effect of $CO_2$

The results show that $J_c$ decreases with an increase in $CO_2$ content in the sintering atmosphere, implying that

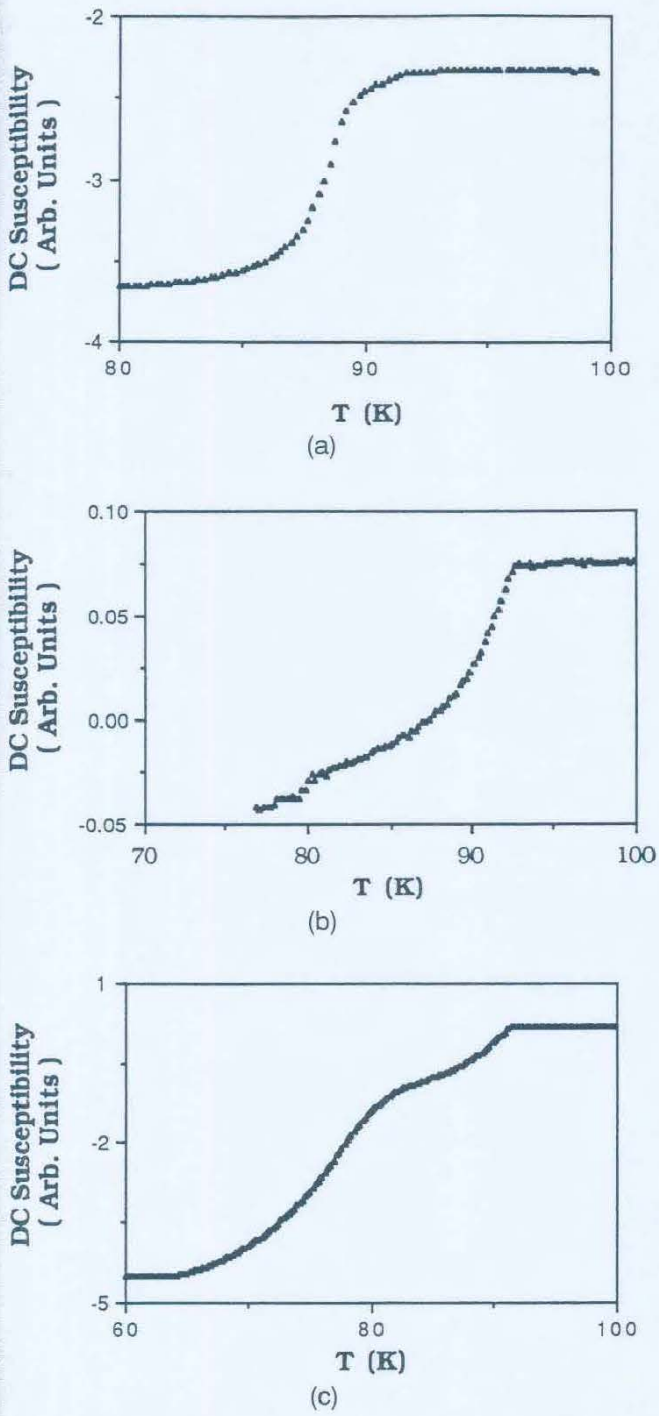


FIG. 9. R.F. susceptibility versus temperature for samples sintered at 940 °C, with (a) pure $O_2$, (b) $O_2$ + 50 ppm $CO_2$, and (c) $O_2$ + 0.5% $CO_2$.

$CO_2$ plays a critical role in the phase relationships in the Y–Ba–Cu–O system. $CO_2$ was also found to lower the decomposition temperature of 123. As the $CO_2$ content in the atmosphere increased, there was clear evidence of an increasing fraction of the $BaCuO_2$, CuO, and $Y_2BaCuO_5$ secondary phases.


FIG. 10. Sample sintered at 970 °C in 0.5% $CO_2$ + 99.5% $O_2$. TEM micrograph for the grain boundary, as marked by G.B., which is wet by a layer of $BaCuO_2$ second phase.

Available phase diagram information[13] shows that 123 melts incongruently at ≈1000 °C in air and forms a liquid and 211. The reverse reaction occurs as the temperature is decreased. The 211 phase and the liquid phase must coexist for the growth of the 123 phase. Once the 211 phase is trapped inside the 123 phase and separated from the liquid phase no more reaction occurs, and 211 will show up as a second phase with the 123 grains. During further cooling, there is a small variation in stoichiometry in the direction of $BaCuO_2$ + CuO, since the 211 phase is trapped inside the 123 phase. Because of the occurrence of local variations in stoichiometry,


FIG. 11. Sample sintered at 970 °C in 0.5% CO + 99.5% $O_2$. HRTEM image of a grain boundary (G.B.) whose normal is [001]. The lattice fringes of 1.19 nm spacing correspond to the tetragonal structure (T), while the lattice fringes of 1.17 nm spacing correspond to the orthorhombic structure (O).

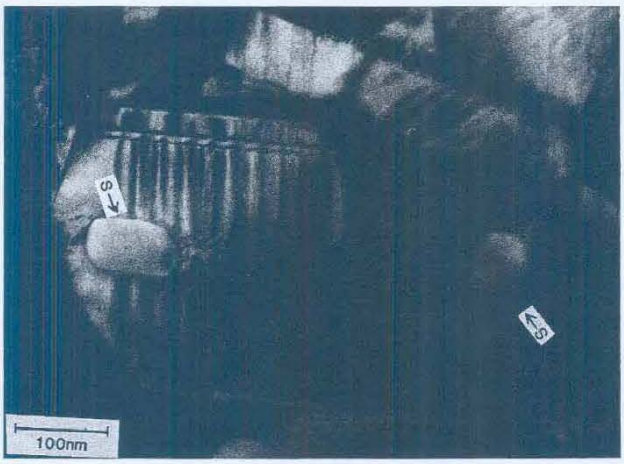


FIG. 12. TEM micrograph of sample sintered in 0.5% $CO_2$ + $O_2$. The second phases, marked S, were identified to be $Y_2BaCuO_5$.

the eutectic reaction takes place and $BaCuO_2$ and CuO form at the grain boundaries.

The decomposition at the grain boundaries weakens the path for the current, thereby decreasing the overall $J_c$ value. The wetting of the boundaries with non-superconducting phases decreases the effective contact area between the superconducting grains and therefore decreases $J_c$. From the data shown in Fig. 10, the width of the second phase region along the grain boundaries was determined to be approximately 50 nm, which is much larger than the coherence length in this material.[14] Therefore, it is reasonable to conclude that these second phases block the passage of currents.

The finding that higher $CO_2$ partial pressures can be tolerated at higher sintering temperatures is thermodynamically consistent. The interaction of 123 with $CO_2$ can be represented by the following reaction:

$$2YBa_2Cu_3O_{6+x}\ (s) + 3CO_2\ (g) \rightarrow Y_2BaCuO_5\ (s) + 3BaCO_3\ (s) + 5CuO\ (s) + xO_2\ (g) \quad (8)$$

The Gibbs free energy change, $\Delta G$, for this reaction can be expressed as follows:

$$\Delta G = \Delta G^\circ + RT\ \ln\left\{(p_{O_2})^\delta/(p_{CO_2})^3\right\} \quad (9)$$

Since $p_{O_2} \approx 1$ atm, and $0 < \delta < 0.5$, the above equation can be simplified as follows:

$$\Delta G = \Delta G^\circ - 3RT\ \ln\ p_{CO_2} \quad (10)$$

At equilibrium, $\Delta G = 0$, and therefore:

$$\Delta G^\circ = 3RT\ \ln\ p_{CO_2} \quad (11)$$

For values of $p_{CO_2} < 1$, $T$ must increase as $p_{CO_2}$ increases in order to maintain the same value of $\Delta G^\circ$. Therefore, increasing the temperature results in a higher $p_{CO_2}$.

The manner in which $CO_2$, contained in the sintering atmosphere, reacts with the bulk material is obviously extremely important. As pointed out at the beginning of this paper, two sources of $CO_2$ are the decomposition of $BaCO_3$ during calcination and/or the $CO_2$ contained in the $O_2$ gas used during sintering and annealing. An additional potential source is the organic binders that are used in the formulation of 123 compounds. The $CO_2$ formed by the interaction of the organic binders and the oxygen from the atmosphere could have a deleterious effect on the performance capabilities of the final product.

Sintering temperatures can be lowered if $p_{CO_2}$ can be lowered, and one expedient means of doing this is to remove the $CO_2$ contained in the $O_2$ gas. The $CO_2$ content of $O_2$ gas varies, depending upon the purity of the gas purchased. While research purity oxygen gas, with a minimum purity of 99.998%, is reported to have a $CO_2$ content of less than 0.1 ppm,[15] commercial purity $O_2$ gas could have a significantly higher $CO_2$ content. Therefore, when using oxygen gas of uncertain $CO_2$ content, it is recommended that a $CO_2$ removal system, such as LiOH, be incorporated in the experimental equipment.

## V. CONCLUSIONS

The present study has shown that 123 compounds can be successfully prepared, from $BaCO_3$ and other oxides, only under conditions to the left of the equilibrium boundary in Fig. 4. The critical current density and transition temperature both depend strongly on the sintering conditions, particularly the partial pressure of $CO_2$ and temperature. The 123 compound reacts with $CO_2$, resulting in compositional inhomogeneity which accumulates at grain boundaries, thereby impeding the current path.

The tendency of the 123 compound to react with $CO_2$ also depends on the sintering temperature; increasing temperatures raise the equilibrium $CO_2$ partial pressure.

## ACKNOWLEDGMENTS

This work was conducted at Argonne National Laboratories and was supported by the United States Department of Energy, Conservation and Renewable Energy, as part of a program to develop electric power technology, and the Office of Basic Energy Sciences, Materials Science, under Contract No. W-31-109-Eng-38; and by the National Science Foundation (DMR 8809854) through the Science and Technology Center for Superconductivity.

## REFERENCES

1. H. Fjellvåg, P. Karen, A. Kjekshus, P. Kofstad, and T. Norby, Acta Chem. Scand. A **42**, 178 (1988).

2. J. D. Jorgensen, M. A. Beno, D. G. Hinks, L. Soderholm, K. J. Volin, R. L. Hitterman, J. D. Grace, I. K. Schuller, C. U. Serge, K. Zhang, and M. S. Kleefish, Phys. Rev. B **36**, 3608 (1987).
3. J. D. Jorgensen, B. W. Veal, W. K. Kwok, G. W. Crabtree, A. Umezawa, L. J. Nowicki, and A. P. Paulikas, Phys. Rev. B **36**, 5731 (1987).
4. W. K. Kwok, G. W. Crabtree, A. Umezawa, B. W. Veal, J. D. Jorgensen, S. K. Malik, L. J. Nowicki, A. P. Paulikas, and L. Nunez, Phys. Rev. B **37**, 106 (1988).
5. U. Balachandran, R. B. Poeppel, J. E. Emerson, S. A. Johnson, M. T. Lanagan, C. A. Youngdahl, D. Shi, K. C. Goretta, and N. G. Eror, Mater. Lett. **8** (11, 12), 454–456 (1989).
6. Y. Syono, M. Kikuchi, K. Ohishi, K. Hiraga, H. Arai, Y. Matsui, N. Kobayashi, T. Sasaoka, and Y. Muto, Jpn. J. Appl. Phys. **26**, L498 (1987).
7. Z. Z. Wang, J. Clayhild, N. P. Ong, J. M. Tarascon, L. H. Green, W. R. McKinnon, and G. W. Hull, Phys. Rev. B **36**, 7222 (1987).
8. Y. Nakazawa and M. Ishikawa, Physica C **158**, 381 (1989).
9. R. S. Kwok, S. W. Cheong, J. D. Thompson, Z. Fisk, J. L. Smith, and J. O. Willis, Physica C **152**, 240 (1988).
10. R. A. Laudise, L. F. Schneemeyer, and R. L. Barnes, J. Cryst. Growth **85**, 569 (1987).
11. R. J. Cava, B. Batlogg, C. H. Chen, E. A. Rietman, S. M. Zahurak, and D. Werder, Phys. Rev. B **36**, 5719 (1987).
12. G. Van Tendeloo, H. W. Zandbergen, and S. Amelinckx, Solid State Commun. **63**, 389 (1987).
13. R. A. Laudise, *op. cit.*
14. T. K. Worthington, W. J. Gallagher, and T. R. Dinger, Phys. Rev. Lett. **59**, 1160 (1987).
15. Matheson Gas Products Catalog (March 1990), p. 41.